Progress In Electromagnetics Research Letters, Vol. 108, 93–102, 2023

Beam Scanning 10×10 Phased Array Antenna Using Liquid Crystal Phase Shifters

Wei Hu[1], Di Jiang[1], Weiyi Yang[1], Pengbo Pan[1], Tianming Bai[1, *], Weiyi Zhang[1], Zhiyong Guo[1], and Guofu Wang[2]

Abstract—In this paper, we devise a phased array antenna with liquid crystal material, employing a 10×10 uniform rectangular array. The phase of the phased array antenna is controlled by loading bias voltage on the liquid crystal layer, and the FoM (figure-of-merit) of the phase shifter can attain $70.6°$/dB. The phased array antenna works at 16 GHz and employs a microstrip circular patch as the radiation unit. The proposed phased array can achieve a gain of 23.1 dBi, and its beam scanning range reaches $\pm 45°$ in simulation experiment. The preliminary measurement results demonstrate that the performance of the proposed antenna is basically consistent with simulation results.

1. INTRODUCTION

Recently, the development of electronic information technology has put forward higher requirements for antenna design. Exploring new antenna design methods and ideas has become one of the current research hotspots [1–3]. Phased array antenna has the functions of beam scanning, beam control, and anti-jamming. It plays an important role in vehicle radar, satellite radar, 5G mobile terminal, and other fields. Therefore, it is widely studied as a representative of high-performance antenna [4–6]. In [7], a 1×4 passive subarray working in Ka band is introduced, which can scan the beam in the range of $\pm 38°$. It is characterized by using BLT (Barium Lanthanide Tetratitanates) material as dielectric plate and phase shift control. As the key component of the phased array antenna, phase shifter can be divided into digital and continuous phase shifters. The design of a digital phase shifter is relatively mature [8–10], but its phase shift value is discrete. Moreover, the cost and volume of the digital phase shifter increase rapidly as the phase shift accuracy improves. The phase shift value of the continuous phase shifter varies continuously in the range of $[0°, 360°]$, which is a better choice for the development of the phased array antenna [11, 12]. Among them, liquid crystal materials have unique advantages, and their dielectric loss decreases with the increase of frequency. Their permittivity can be changed by external electric or magnetic field, so as to realize the regulation of transmission phase [13]. Several microwave components based on liquid crystal material have been developed, including filter, lens antenna [14], reflective array antenna [15], etc. Phased array antenna has broad application prospects in modern wireless communication systems. However, there are few reports on the reconfigurable performance of phased array antenna using new tunable materials such as liquid crystal. In this paper, the phase shifter is designed using liquid crystal materials to control the beam of a phased array antenna, which expands the application of liquid crystal materials in the microwave field and provides a new solution for the reconfigurable phased array antenna. Compared with the traditional microwave components, liquid crystal material-based devices have lower profile, lighter weight, and continuous tuning [16].

Received 17 August 2022, Accepted 20 December 2022, Scheduled 6 January 2023
* Corresponding author: Tianming Bai (tianyumingfeng@163.com).
[1] Information and Communication Engineering, University of Electronic Science and Technology of China, Chengdu 611731, China.
[2] Information and Communication Engineering, Guilin University of Electronic Technology, Guilin, China.

In this paper, a phased array antenna based on liquid crystal materials is studied. By simulating the unit and arrays of Ansoft HFSS, a 10×10 uniformly rectangular microstrip phased array antenna working in Ku band is proposed, and its performance is verified by fabrication and measurement.

2. LIQUID CRYSTAL PHASE SHIFTER DESIGN

A meander transmission line is adopted for design, and the structural diagram of phase shifter is shown in Fig. 1. The parameters of phase shifter unit are shown in Table 1. The overall structure is composed of three substrates. The middle substrate is grooved to contain liquid crystal, and the upper and lower substrates are used for packaging and fixing. The transmission line is partially above the liquid crystal and forms a bias electrode with the lower metal. To realize the miniaturization design, the transmission line is set to d_1 and connected with a d_2 line for impedance matching. The permittivity of liquid crystal is controlled by changing the potential differences among them, so as to realize phase-shifting control.

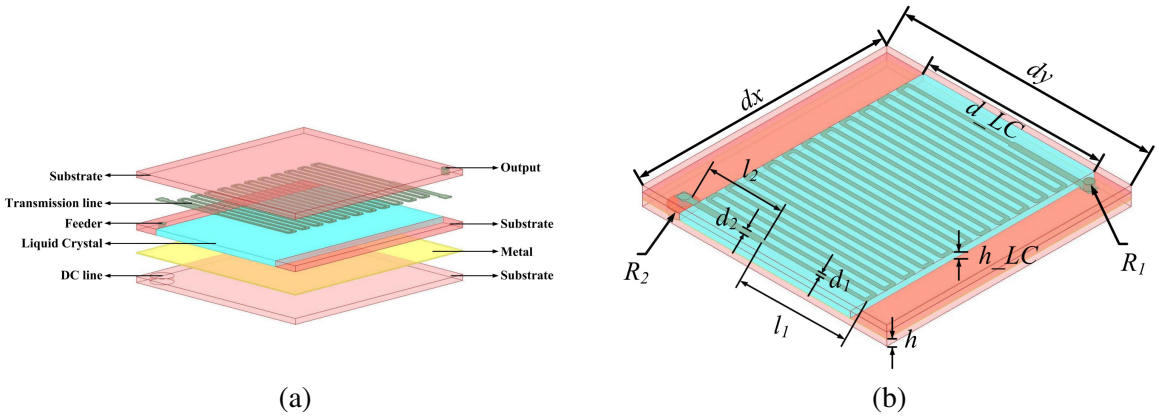

Figure 1. Structure diagram of liquid crystal phase shifter: (a) Section structure; (b) Schematic diagram of phase shifting structure.

Table 1. Dimension of phase shifter unit.

Parameters	***dx***	***dy***	***h_LC***	$\boldsymbol{d_1}$	$\boldsymbol{d_2}$	***d_LC***
Length (mm)	9.3	9.3	0.254	0.15	0.25	7
Parameters	$\boldsymbol{R_1}$	$\boldsymbol{R_2}$	$\boldsymbol{h}$	$\boldsymbol{l_1}$	$\boldsymbol{l_2}$	
Length (mm)	0.18	0.5	0.254	4.31	3	

The simulation results are shown in Fig. 2. The -10 dB bandwidth range is 4.95 GHz. And the maximum differential phase shift curve is plotted in Fig. 3. The phase shift exceeds 360° in the frequency range of 15 GHz–18 GHz, with good linearity, which is convenient to control the phase shift.

A key index of phase shifter is figure of merit (FoM), which is defined as the ratio of the maximum differential phase shift to the highest IL over all tuning states.

$$\text{FoM} = \frac{\Delta\phi_{\max}}{\text{IL}_{\max}} \, (^\circ/\text{dB}). \tag{1}$$

The FoM simulation results of the designed liquid crystal phase shifter are shown in Fig. 4, and the comparison results with other phase shifters are listed in Table 2.

3. DESIGN OF PHASED ARRAY UNIT

Microstrip patch antenna is utilized as the phased array antenna unit. To facilitate independent control, coaxial feed is used for back feed, so as to realize the connection of multi-layer structure. The phase

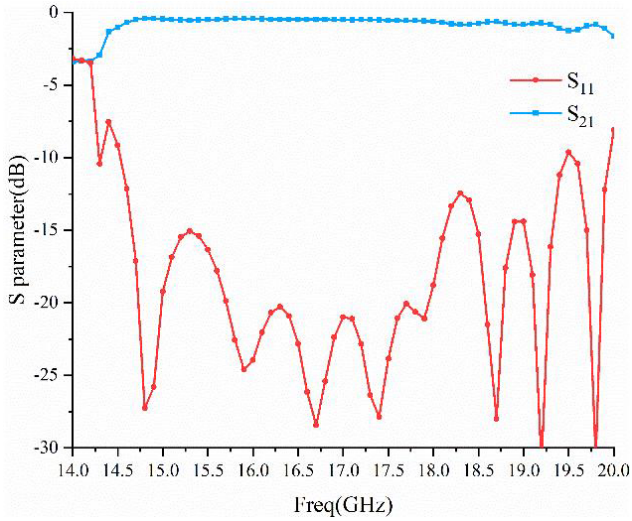

Figure 2. S parameters of phase shifter.

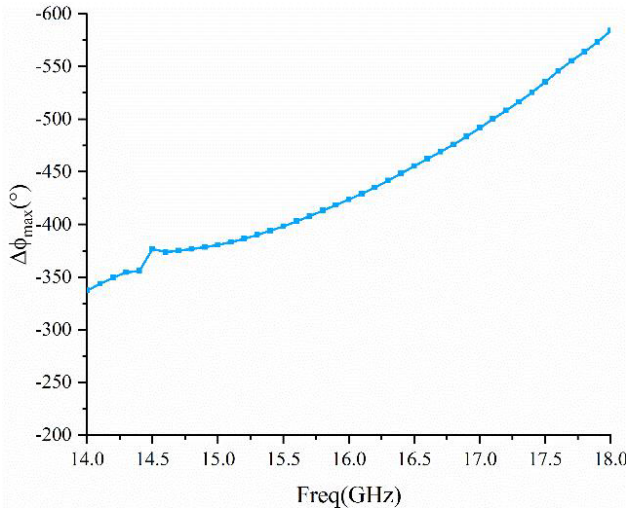

Figure 3. Simulated differential phase shift.

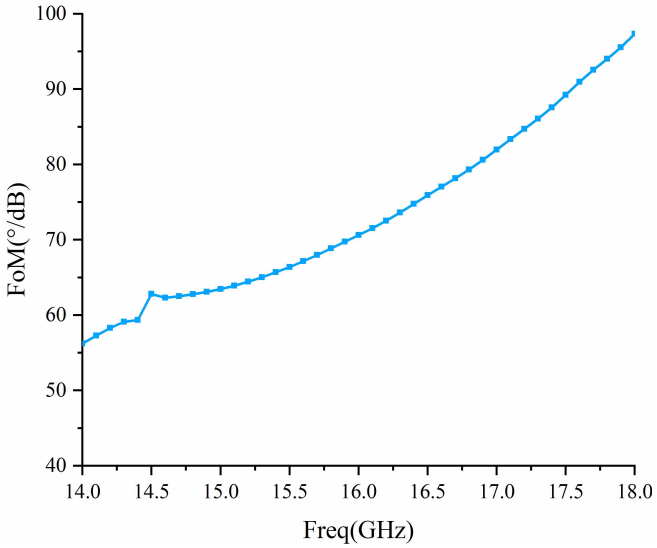

Figure 4. Simulation results of FoM.

Table 2. Comparison of liquid crystal phase shifters.

Ref.	Freq. (GHz)	FoM (°/dB)	S_{11} (dB)
[16]	17.5	63	< -15
[17]	28.4	54	< -20
This work	16	70.6	< -10

shifter is combined with the radiation unit to form a phase control unit, and the uppermost layer is a circular radiation patch. The substrate of the middle layer is grooved to carry the liquid crystal, and the upper and lower substrates (Rogers 5880) are bonded with the substrate of the middle layer. Below the liquid crystal material is a metal layer, and an external bias line is connected with the metal layer. When the liquid crystal layer is loaded with bias voltage, the permittivity of liquid crystal can be altered, and then the phase control can be realized through the bending transmission line. The radiation

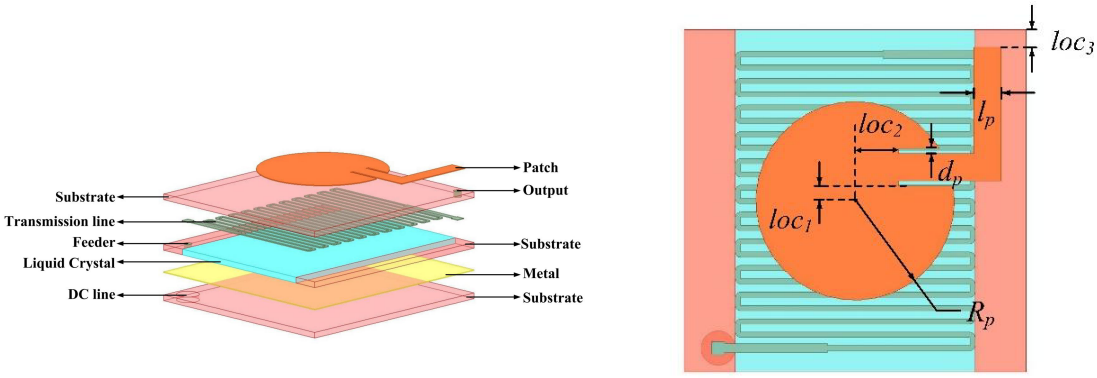

Figure 5. Structure diagram of phased array unit: (a) Section structure; (b) Schematic of the unit.

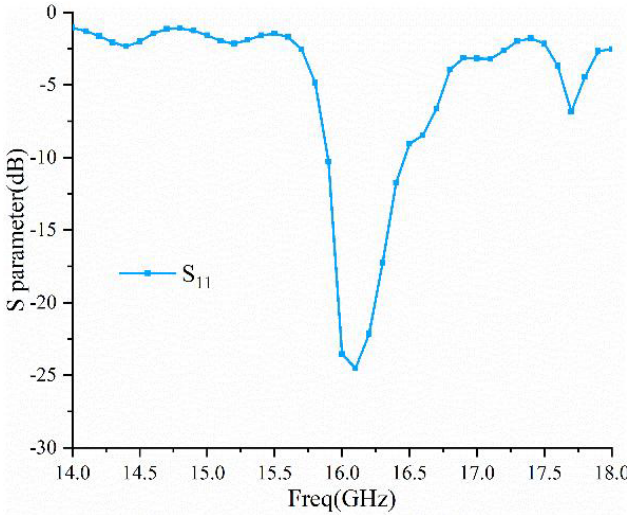

Figure 6. S parameter of phase array unit.

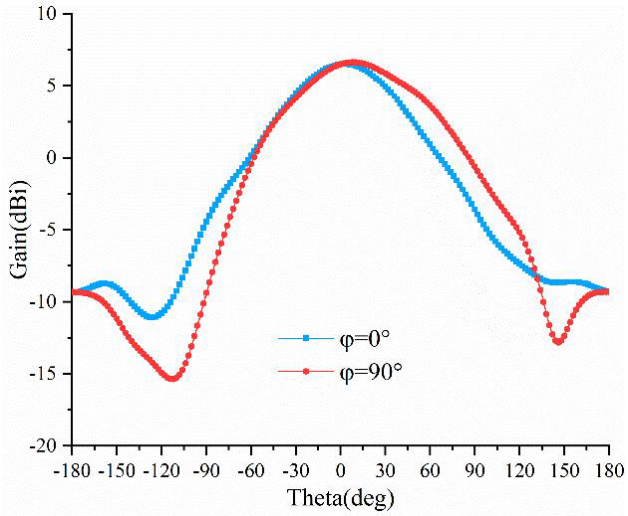

Figure 7. Gain of phase array unit.

patch and transmission line are placed on both sides of the same substrate. The corresponding model is presented in Fig. 5, while the dimensions of antenna unit are listed in Table 3.

The simulation results obtained after optimizing the relevant parameters according to the structure are shown in Fig. 6 and Fig. 7. S_{11} is lower than -10 dB in the range of 15.9 GHz–16.5 GHz. Since the microstrip patch antenna is narrow-band, the bandwidth is greatly reduced compared to the phase shifter. The gain of the center frequency (16 GHz) is 6.6 dBi.

Table 3. Dimension of antenna unit.

Parameters	dp	lp	R_p	loc_1	loc_2	loc_3
Length (mm)	0.15	0.8	2.9	0.43	1.27	0.52

4. DESIGN OF PHASED ARRAY

The phased array is designed as a 10×10 rectangular uniform array. The simulation model is shown in Fig. 8. The upper layer is perforated to facilitate liquid crystal filling. The lower metal of the liquid

Figure 8. Simulation model of 10 × 10 liquid crystal phased array.

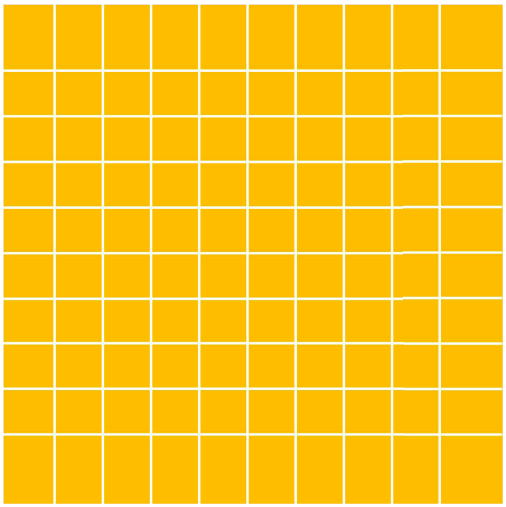

Figure 9. Liquid crystal bias loaded metal layer.

crystal layer is separated so that the bias voltage loaded to the unit can be independently controlled, as depicted in Fig. 9.

The simulation results of the proposed array antenna are displayed in Fig. 10. The main beam gain can reach 24.8 dBi, and the half beam width is about 12°, which is consistent with the expected results.

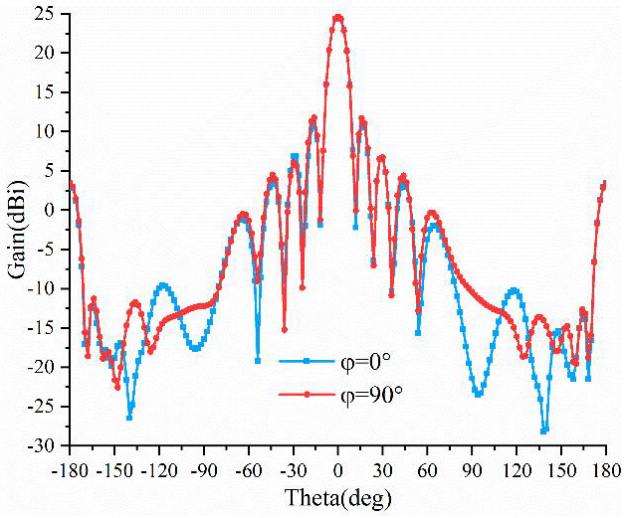

Figure 10. Simulation results of array antenna gain.

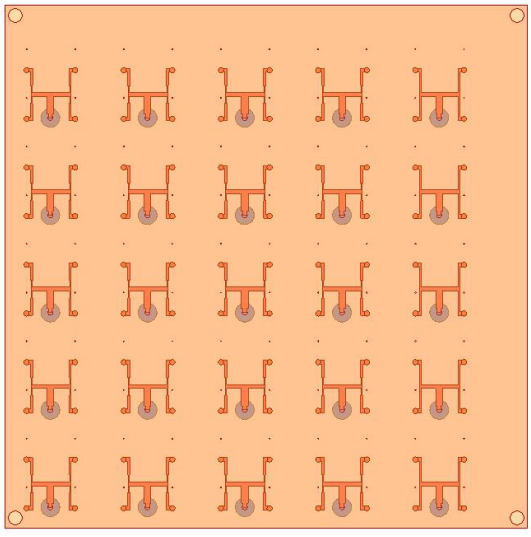

Figure 11. Structure of power division feed array.

To reduce the number of feed cables, a power distributor array is utilized to feed each unit. Since the phased array has a size of 10 × 10, after comprehensive consideration, 25 four-channel power divider feeding structures are used for equal amplitude and in-phase feeding. The power divider array feeding structure is shown in Fig. 11. The sectional structure of the phased array antenna with power division layer is illustrated in Fig. 12.

The simulation result of array antenna gain after adding the feed network to the phased array is shown in Fig. 13, where the peak gain reaches 23.1 dBi.

To simulate the beam deflection of phased array, the simulation is conducted according to the beam

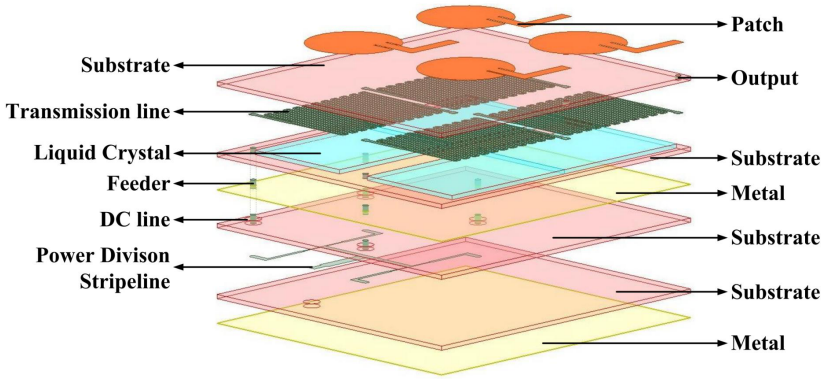

Figure 12. Sectional structure of phased array antenna with power division layer.

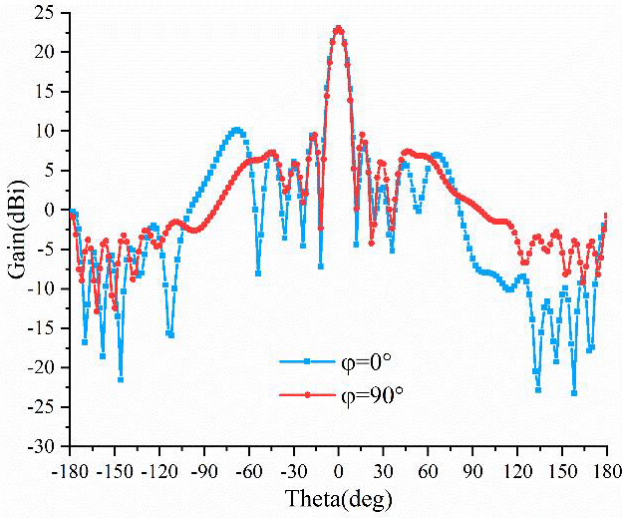

Figure 13. Simulation results of array antenna gain.

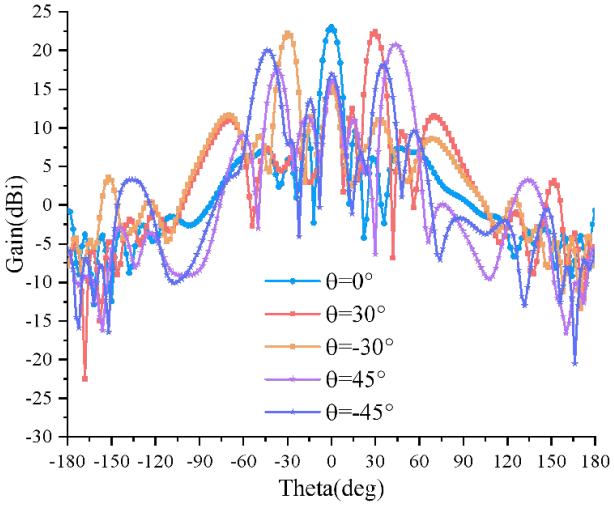

Figure 14. Simulation results of beam scanning.

deflection theory of phased array.

Via theory of phased array [18], to achieve beam scanning in one dimension, the radiation field of a phased array can be seen as N elements arranged in a row with a spacing of d, where its phase difference of adjacent elements is ζ. Its radiation field can be expressed as

$$E_\theta = E_m \frac{F_{\text{element}}(\theta,\varphi)}{r} e^{-jkt} \sum_{i=0}^{N-1} e^{ji(kd\cos\phi+\zeta)} = E_m N \frac{e^{-jkr}}{r} F_{\text{element}}(\theta,\varphi) f(\theta,\varphi) \tag{2}$$

where $f(\theta,\varphi) = \frac{1}{N}\sum_{i=0}^{N-1} e^{ji(kd\cos\phi+\zeta)}$, $\cos\phi = \sin\theta\cos\varphi$.

Thus, the pattern function of an array can be expressed as

$$F(\theta,\varphi) = F_{\text{element}}(\theta,\varphi) f(\theta,\varphi) \tag{3}$$

Using the sum of equal series, the matrix factor can be simplified to

$$f(\theta,\varphi) = \frac{1}{N}\sum_{i=0}^{N-1} e^{ji\psi} = \frac{\sin\frac{N\psi}{2}}{N\sin\frac{\psi}{2}} \tag{4}$$

where $\psi = kd\cos\phi + \zeta$.

When $kd\cos\phi_m + \zeta = 0$ ($\psi = 0$), the radiation direction is maximum. To achieve beam radiation in the direction of ϕ_m, the phase difference between the different elements is

$$\zeta = -kd\cos\phi_m \tag{5}$$

The beam deflection simulation results are shown in Fig. 14, where a beam scanning range of $[-45°, +45°]$ can be realized. θ is the beam scanning angle in the dimension.

The comparison with phased arrays fabricated by other methods is displayed in Table 4.

5. FABRICATION AND MEASUREMENT

The designed phased array antenna is fabricated and measured, as depicted in Fig. 15.

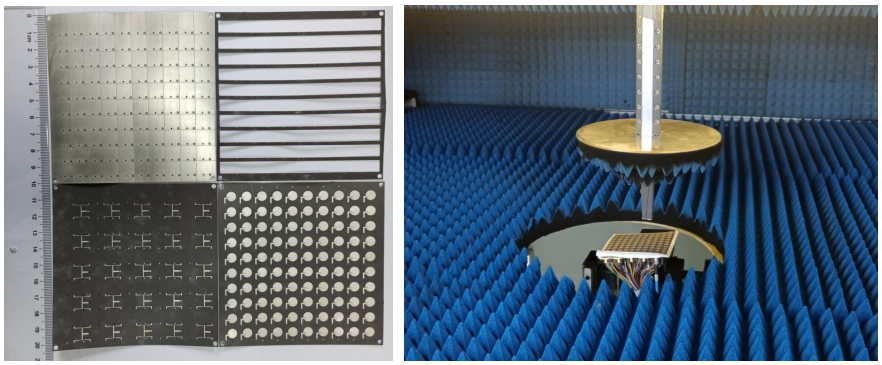

(a) (b)

Figure 15. (a) Fabricated prototype of the proposed array. (b) Antenna array under measurement.

As shown in Fig. 16, this design includes 25 feed ports, each of which can excite a branch of 2×2 units. Due to limited test conditions, we do not have a 25-channel power divider. Therefore, we measured a 2×2 branch in the center of the array. The comparison of simulation and measurement results of the designed antenna is shown in Fig. 17. It is observed that the measured peak gain is 10 dBi, which is 0.5 dB lower than the simulation results.

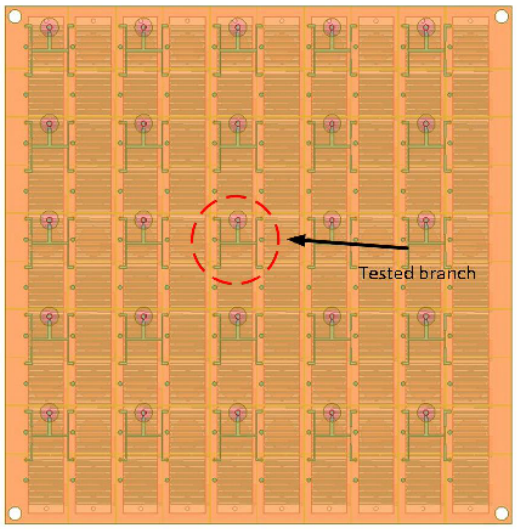

Figure 16. Back of the antenna.

Table 4. Comparison with other phased arrays.

Ref.	Tuning Material	Peak Gain (dBi)	Scanning Range	Array Size
[11]	BST	12.5	1D, ±30°	1 × 4
[19]	BST	8.1	1D, ±25°	4 × 4
[20]	BST	< 14	1D, ±30°	1 × 4
[16]	LC	5.9	2D, ±25°	2 × 2
[17]	LC	4.5	1D, ±40°	1 × 4
This work	LC	23.1	1D, ±45°	10 × 10

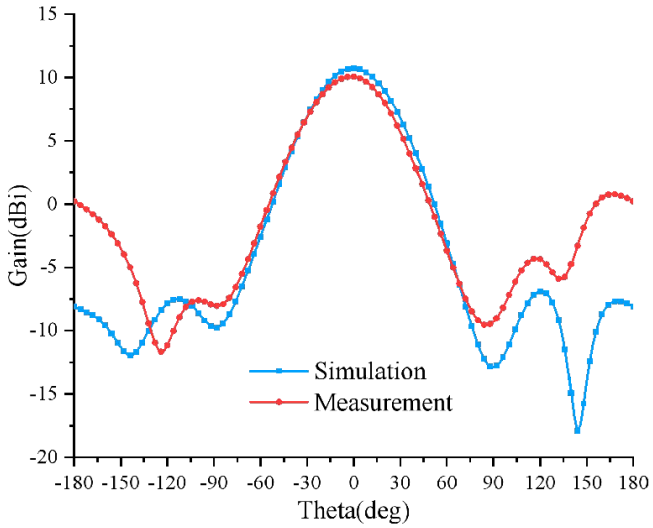

Figure 17. Comparison results of measurement and simulation gain.

6. CONCLUSION

In this paper, a 10 × 10 phased array antenna with liquid crystal materials and electronically controlled scanning is designed. The designed antenna can achieve a peak gain of 23 dBi, and its scanning range can reach ±45° in simulation. During the antenna measurement, we only tested some of the branches due to the lack of components. The test results demonstrate that the performance of the proposed antenna is basically consistent with the simulation results.

ACKNOWLEDGMENT

This work was supported by Sichuan Science and Technology Program (2022YFG0117, 2022YFQ0088); Funding of GF Science and Technology Key Laboratory (612502200303); the Fundamental Research Funds for the Central Universities (ZYGX2019J007); Sichuan Province Outstanding Young Science and Technology Talent Project (2021JDJQ0026).

REFERENCES

1. Duncombe, J. U., "Infrared navigation — Part I: An assessment of feasibility," *IEEE Trans. Electron Devices*, Vol. 11, No. 1, 34–39, Jan. 1959.

2. Yang, X., Y. Liu, H. Lei, Y. Jia, P. Zhu, and Z. Zhou, "A radiation pattern reconfigurable Fabry-Pérot antenna based on liquid metal," *IEEE Transactions on Antennas and Propagation*, Vol. 68, No. 11, 7658–7663, Nov. 2020.
3. Chen, Z., H.-Z. Li, H. Wong, X. Zhang, and T. Yuan, "A circularly-polarized-reconfigurable patch antenna with liquid dielectric," *IEEE Open Journal of Antennas and Propagation*, Vol. 2, 396–401, 2021.
4. Ibrahim, M. I., M. G. Ahmed, M. El-Nozahi, A. M. E. Safwat, and H. El-Hennawy, "Design and performance analysis of a miniature, dual-frequency, millimeter wave linear phased array antenna," *IEEE Transactions on Antennas and Propagation*, Vol. 65, No. 12, 7029–7037, Dec. 2017.
5. Moon, S., S. Yun, I. Yom, and H. L. Lee, "Phased array shaped-beam satellite antenna with boosted-beam control," *IEEE Transactions on Antennas and Propagation*, Vol. 67, No. 12, 7633–7636, Dec. 2019.
6. Syrytsin, I., S. Zhang, G. F. Pedersen, and A. S. Morris, "Compact quad-mode planar phased array with wideband for 5G mobile terminals," *IEEE Transactions on Antennas and Propagation*, Vol. 66, No. 9, 4648–4657, Sept. 2018.
7. Al-Saedi, H., S. Gigoyan, W. M. Abdel-Wahab, et al., "A low-cost Ka-band circularly polarized passive phased-array antenna for mobile satellite applications," *IEEE Transactions on Antennas and Propagation*, Vol. 67, No. 1, 221–231, Jan. 2019.
8. Koh, K. and G. M. Rebeiz, "0.13-µm CMOS phase shifters for X-, Ku-, and K-band phased arrays," *IEEE Journal of Solid-State Circuits*, Vol. 42, No. 11, 2535–2546, Nov. 2007.
9. Jeon, H. and K. W. Kobayashi, "A high linearity +44.5-dBm IP3 C-band 6-bit digital phase shifter using SOI technology for phased array applications," *IEEE Microwave and Wireless Components Letters*, Vol. 29, No. 11, 733–736, Nov. 2019.
10. Tsai, J.-H., Y.-L. Tung, and Y.-H. Lin, "A 27–42-GHz low phase error 5-bit passive phase shifter in 65-nm CMOS technology," *IEEE Microwave and Wireless Components Letters*, Vol. 30, No. 9, 900–903, Sept. 2020.
11. Nikfalazar, M., C. Kohler, A. Wiens, et al., "Beam steering phased array antenna with fully printed phase shifters based on low-temperature sintered BST-composite thick films," *IEEE Microwave and Wireless Components Letters*, Vol. 26, No. 1, 70–72, Jan. 2016.
12. Chen, C. Y., C. F. Hsieh, Y. F. Lin, R. P. Pan, and C. L. Pan, "Magnetically tunable room-temperature 2π liquid crystal terahertz phase shifter," *Opt. Exp.*, Vol. 12, No. 12, 2630–2635, Jun. 2004.
13. Woehrle, C. D., D. T. Doyle, S. A. Lane, and C. G. Christodoulou, "Space radiation environment testing of liquid crystal phase shifter devices," *IEEE Antennas and Wireless Propagation Letters*, Vol. 15, 1923–1926, 2016.
14. Polat, E., R. Reese, M. Jost, et al., "Tunable liquid crystal filter in nonradiative dielectric waveguide technology at 60 GHz," *IEEE Microwave and Wireless Components Letters*, Vol. 29, No. 1, 44–46, Jan. 2019.
15. Perez-Palomino, G., M. Barba, J. A. Encinar, et al., "Design and demonstration of an electronically scanned reflectarray antenna at 100 GHz using multiresonant cells based on liquid crystals," *IEEE Transactions on Antennas and Propagation*, Vol. 63, No. 8, 3722–3727, Aug. 2015.
16. Karabey, O. H., A. Gaebler, S. Strunck, and R. Jakoby, "A 2-D electronically steered phased-array antenna with 2×2 elements in LC display technology," *IEEE Transactions on Microwave Theory and Techniques*, Vol. 60, No. 5, 1297–1306, May 2012.
17. Wang, D., E. Polat, H. Tesmer, R. Jakoby, and H. Maune, "A compact and fast 1×4 continuously steerable endfire phased-array antenna based on liquid crystal," *IEEE Antennas and Wireless Propagation Letters*, Vol. 20, No. 10, 1859–1862, Oct. 2021, doi: 10.1109/LAWP.2021.3096035.
18. Kraus, J. D. and R. J. Marhefka, *Antennas: For All Applications*, 3rd Edition, 2006.
19. Nikfalazar, M., M. Sazegar, A. Mehmood, et al., "Two-dimensional beam-steering phased-array antenna with compact tunable phase shifter based on BST thick films," *IEEE Antennas and Wireless Propagation Letters*, Vol. 16, 585–588, 2017.

20. Nikfalazar, M., A. Mehmood, M. Sohrabi, and M. Mikolajek, "Steerable dielectric resonator phased-array antenna based on inkjet-printed tunable phase shifter with BST metal-insulator-metal varactors," *IEEE Antennas and Wireless Propagation Letters*, Vol. 15, 877–880, 2016.